Chinese Chemical Letters 37 (2026) 111793

Contents lists available at ScienceDirect

Chinese Chemical Letters

journal homepage: www.elsevier.com/locate/cclet

Asymmetric catalysis for the synthesis of planar chiral ferrocene derivatives

Haitao Liu, Youlin Deng, Dan Ling, Lingzhu Chen*, Zhichao Jin*

State Key Laboratory of Green Pesticide, Guizhou University, Guiyang 550025, China

ARTICLE INFO

Article history:
Received 20 May 2025
Revised 19 August 2025
Accepted 4 September 2025
Available online 5 September 2025

Keywords:
Ferrocene derivatives
Planar chirality
Asymmetric catalysis
Desymmetrization
Kinetic resolution

ABSTRACT

The asymmetric catalytic synthesis of planar chiral ferrocene derivatives has received dramatic attention in recent years. Transition metal-catalyzed asymmetric cross-coupling reactions and C–H functionalization reactions have played significant roles in the stereoselective construction of planar chiral ferrocene derivatives. Transition metals such as copper, palladium, rhodium, iridium, gold, and platinum have been adopted as the effective catalysts in combination with various chiral ligands to achieve satisfactory yields and stereoselectivity. Organic catalysts have also shown great potential in the synthesis of planar chiral ferrocenes. Chiral amines and *N*-heterocyclic carbenes (NHCs) have been the key catalysts for facile access to multi-functional ferrocene derivatives. Some of the planar chiral ferrocene molecules obtained from the above methods have demonstrated promising applications in the development of novel ligands for asymmetric synthesis and pesticides for plant protection. This review provides an overview on the key progresses in the catalytic synthesis of planar chiral ferrocene derivatives using transition metal catalysts and organic catalysts. The merits, challenges and potential directions in the future development within this highly active research field are also discussed at the end of this review.

© 2025 Published by Elsevier B.V. on behalf of Chinese Chemical Society and Institute of Materia Medica, Chinese Academy of Medical Sciences.

1. Introduction

Ferrocene derivatives have been widely used in material sciences [1–4], organic synthesis [5,6], and pharmaceutical chemistry [7–9] (Scheme 1). For example, ferrocene derivatives have exhibited anticancer [10–15], antimalarial [16], antibacterial [17,18], antifungal and other interesting bioactivities in drug development [19]. Enantio-pure planar chiral ferrocene structures have been extensively used as excellent ligands and catalysts for asymmetric synthesis in both scientific research and industrial production [20–27]. Therefore, the development of efficient and enantioselective catalytic methods for the synthesis of novel planar chiral ferrocene structures has attracted great interest of scientists focusing on various disciplines.

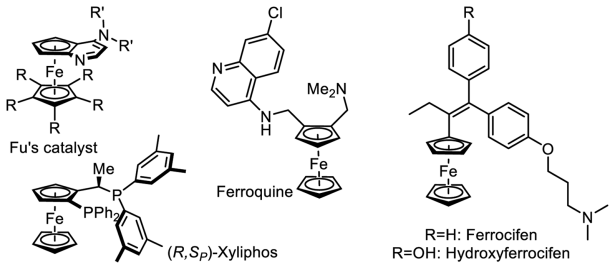
The preparation of optically pure planar chiral ferrocene derivatives has long relied on chiral resolutions [28–31], desymmetrization, enantio– and diastereoselective directed *o*-metalation reactions [32–36]. The last decade has witnessed prosperous development in the enantioselective catalytic methods for the synthesis of various planar chiral ferrocene molecules, with both transition metal complexes and organic molecules used as the chiral catalysts [37]. The asymmetric catalytic methods that have been developed possess certain advantages in the atom economy, environmental friendly and increased synthetic efficiency. It is therefore significant and urgent for scientists to get an overview on the development of catalytic methods for the facile synthesis of planar chiral ferrocene structures. Herein, we aim to provide a systematic summary on the transition metal- and organocatalyzed desymmetrizations and kinetic resolutions that have been developed in the recent decade for the establishment of the planar chirality based on ferrocene structures. The merits, challenges and potential directions in the future development within this highly active research field are also discussed at the end of this review.

2. Transition metal-catalyzed planar chiral ferrocene synthesis

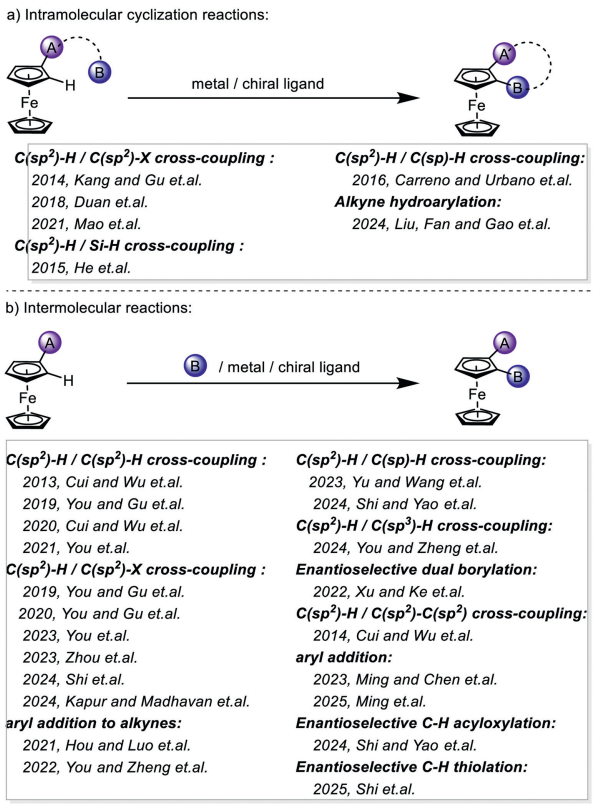
Significant progress has been made in the field of transition metal-catalyzed synthesis of planar chiral ferrocene derivatives (Scheme 2). Various asymmetric cross-coupling reactions and C–H bond activation reactions of ferrocenes have been developed with the catalysis of transition metals, which generally require the introduction of directing groups and the combination of chiral ligands to achieve regio- and stereoselectivity. For example, asymmetric C–H alkylation, C–H vinylation, C–H alkynylation, C–H acylation, C–H borylation, C–H acyloxylation, and C–H thiolation reactions have been adopted to establish planar chiralities on ferrocene

* Corresponding authors.
E-mail addresses: lzchen@gzu.edu.cn (L. Chen), zcjin@gzu.edu.cn (Z. Jin).

https://doi.org/10.1016/j.cclet.2025.111793
1001-8417/© 2025 Published by Elsevier B.V. on behalf of Chinese Chemical Society and Institute of Materia Medica, Chinese Academy of Medical Sciences.



Scheme 1. Representative planar chiral ferrocene derivatives.



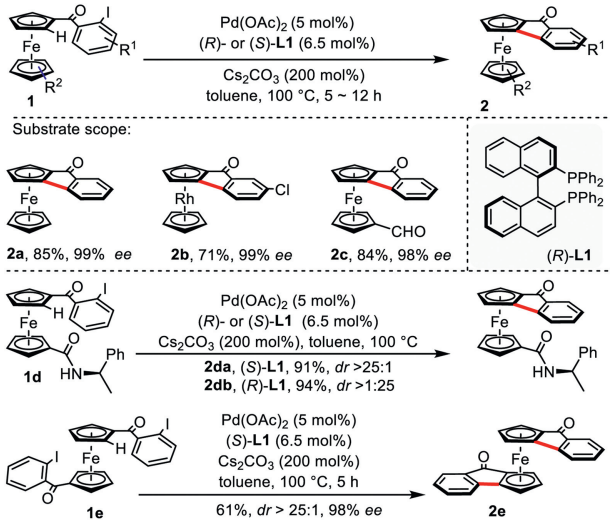
Scheme 2. Transition metal-catalyzed asymmetric synthesis of planar chiral ferrocene derivatives.

frameworks. Pd catalysts and other transition metal catalysts such as Rh, Ir, Au, Pt, Cu, and Co have been explored to expand reaction conditions and substrate scope.

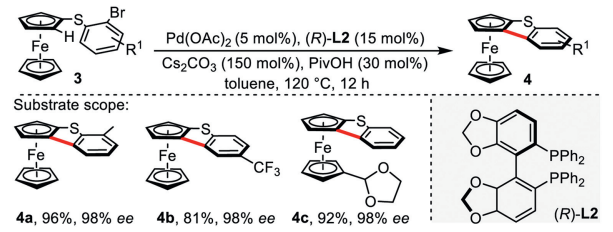
2.1. Intramolecular cyclization reactions

In 2014, Kang and Gu's group achieved the ferrocene-based indanone derivatives **2** through palladium-catalyzed asymmetric cyclization reaction with chiral 1,1′-bi-2,2′-naphthol (BINAP) **L1** used as the ligand (Scheme 3) [38]. The *o*-C-H bond on the cyclopentadienyl ring was coupled with the *o*-C-I bond on the phenyl group, exhibiting excellent diastereo- and enantioselectivity. The reaction featured mild reaction condition and broad substrate scope. Noteworthily, the iron center in the ferrocene structure could also be switched into a ruthenium atom, providing an efficient route for the synthesis of various planar chiral metallocene compounds.

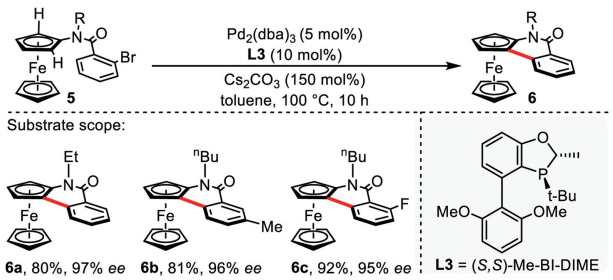
In 2018, Duan and co-workers used as the chiral biaryl-bisphosphine (*R*)-**L2** as the ligand in the Pd-catalyzed enantioselective cyclization of the ferrocene aryl sulfides **3**, affording the ferrocene-derived planar chiral thiophene compounds in good to excellent yields and enantioselectivities (Scheme 4) [39]. The sulfur



Scheme 3. Pd(II)-catalyzed intramolecular cyclization to form indenone derivatives.



Scheme 4. Pd(II)-catalyzed intramolecular cyclization to form planar chiral thiophene compounds.

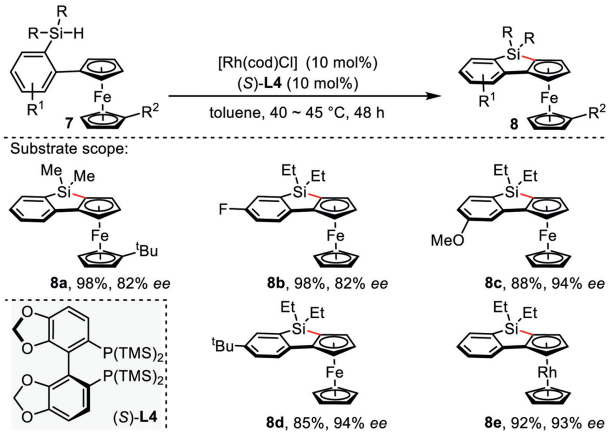


Scheme 5. Pd-catalyzed the intramolecular cyclization to form soquinolinone-fused ferrocenes.

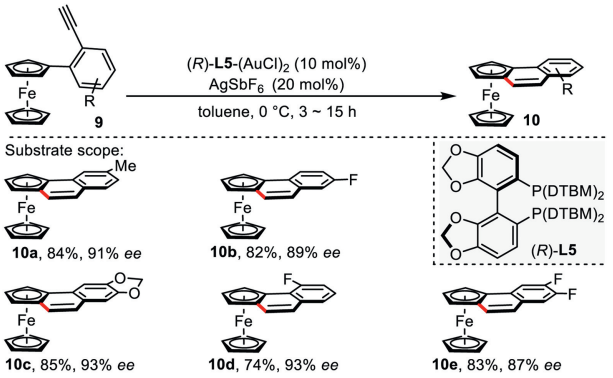
atom in the reaction substrate could be switched into an oxygen atom without much erosion on the reaction outcomes. The current method could also be adopted in the synthesis of the ferrocene-based thiophene compounds bearing two stereogenic planes as single diastereomers.

In 2021, Mao and co-workers reported a Pd-catalyzed desymmetric C–H functionalization of the ferrocene cyclopentadienyl ring with the intramolecular bromophenyl group for enantioselective synthesis of planar chiral isoquinolinone-ferrrocene compounds (Scheme 5) [40]. The chiral **L3** that developed by the Tang's group was used as the ligand [41], with a variety of ferrrocene-based isoquinolinone products afforded in generally good to excellent yields and enantioselectivities under mild conditions.

In 2015, He and co-workers reported a Rh(III)-catalyzed enantio–selective C–H bond silylation reaction of the ferrocenes **7** (Scheme 6) [42]. The chiral diphosphine ligand (*S*)-**L4** was used in combination with the Rh(III) catalyst, and a broad scope of planar chiral ferrocene-fused silole products **8** were afforded in good to excellent yields and optical purity. Noteworthily, the iron center in



Scheme 6. Rh(III)-catalyzed C–H silylation reaction to form planar chiral thiophene compounds.



Scheme 7. Au(I)-catalyzed cycloisomerization to form planar chiral aromatic ferrocene compounds.

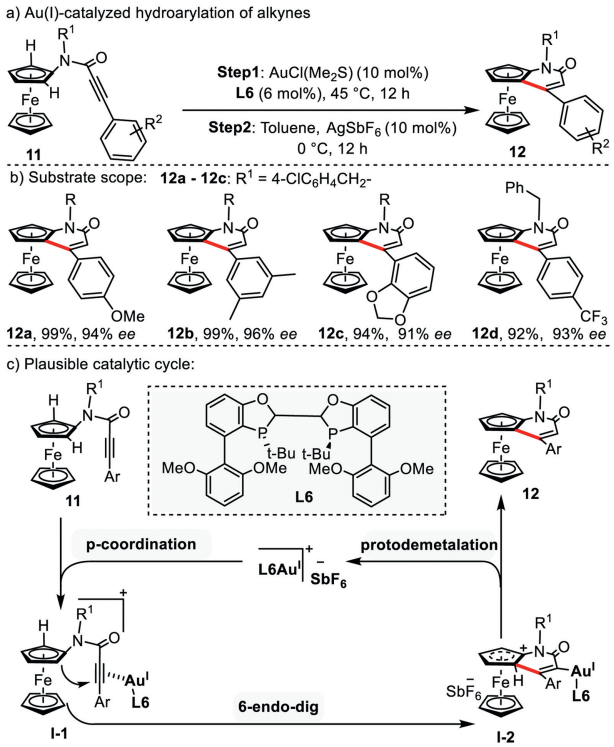
the ferrocene structure can be replaced with a ruthenium atom, offering a versatile and efficient strategy for the synthesis of diverse planar chiral metallocene derivatives.

In 2016, Carreno, Urbano and co-workers developed an Au(I)-catalyzed cycloisomerization of *o*-alkynylaryl ferrocenes **9**, using the selenium-phosphine (*R*)-**L5** as the chiral ligand and $AgSbF_6$ as the halide scavenger (Scheme 7) [43]. A broad scope of planar-chiral aromatic ferrocene products with different substituents were afforded in good to excellent yields and enantioselectivities.

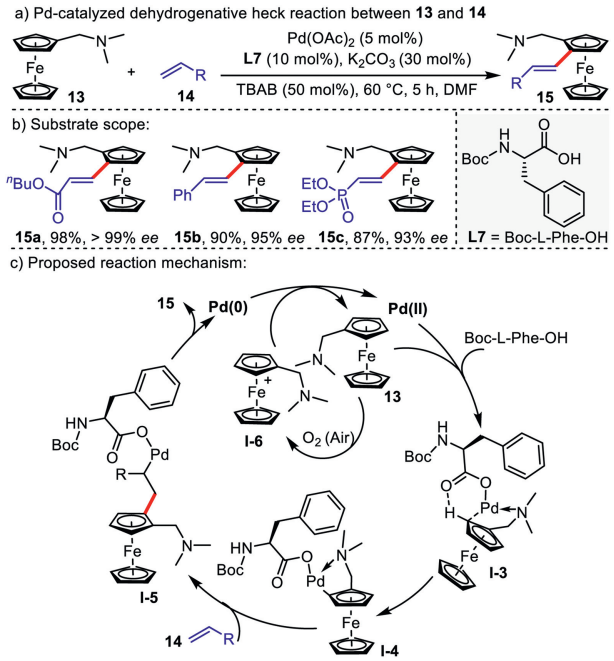
In 2024, Liu, Fan, Gao and co-workers utilized the Tang's bisphosphine **L6** as the ligand to coordinate with the Au(I) catalyst for the desymmetric intramolecular hydroarylation reaction of *N*-ferroceneyl propiolamides (Scheme 8a) [44]. A broad scope of planar chiral ferrocenepyridin-2(1*H*)-one products bearing various substituents on the phenyl moieties were efficiently afforded in good to excellent optical purity. The proposed reaction mechanism is depicted in Scheme 8c. Initially, the chiral gold catalyst formed from the $AuCl(Me_2S)$ and the chiral ligand coordinates with the triple bond of the *N*-ferrocenylpropanylamide substrate to give the chiral Au(I)-π complex **I-1**. The *o*-position of the ferrocene moiety then attacks the π-activated alkyne group through a conjugate addition process to produce the Au(I)-enamide intermediate **I-2**, which then undergoes a protodemetalation step to give the final product **12** and regenerate the Au(I) catalyst for additional catalytic cycles.

2.2. Intermolecular reactions

In 2013, Cui, Wu and co-workers reported an asymmetric dehydrogenative Heck reaction between the *N*,*N*-

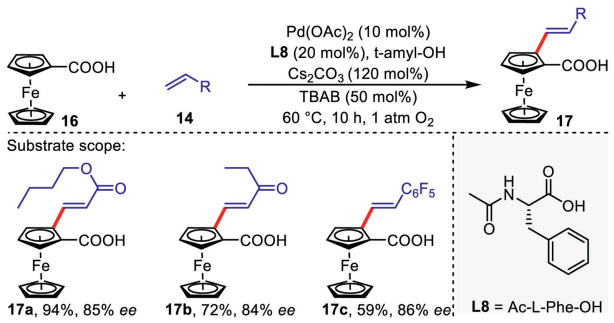


Scheme 8. Au(I)-catalyzed intramolecular cyclization to form planar chiral ferrocenepyridin-2(1*H*)-one products.



Scheme 9. Pd(II)-catalyzed enantioselective alkenylation of *N*,*N*-dimethylaminomethylferrocene.

dimethylaminomethylferrocene **13** and the alkene **14**, with the Pd(II) salt used as the reaction catalyst and the chiral amino acid **L7** used as the chiral ligand (Scheme 9) [45]. A broad scope of functional groups could be tolerated on the alkene **14**, and the planar chiral ferrocenyl phosphine products were facilely achieved in generally excellent optical purity. The proposed reaction mechanism is depicted in Scheme 9c. Initially, the chiral palladium catalyst formed by the Pd(II) salt and the chiral ligand coordinates with the N atom of substrate **13** to give the cyclopalladated com-



Scheme 10. Pd(II)-catalyzed C–H alkenylation reaction between ferrocenecarboxylic acid with alkene.

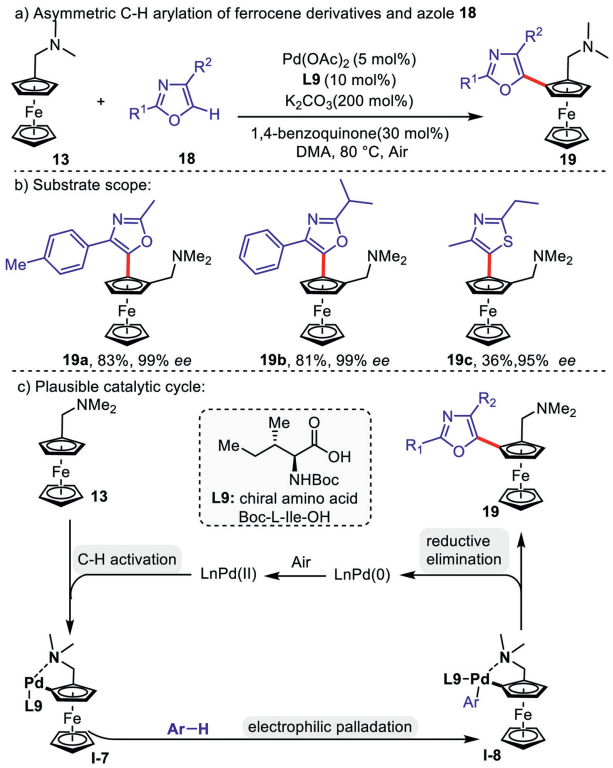
plex **I-3**, and subsequently undergoes enantioselective electrophilic attack at the *o*-position carbon atom (*via* bicycle-intermediate **I-3**) to produce the cyclopalladated complex **I-4**. The cyclopalladated complex **I-4** can be coordinated with alkene **14** under mild conditions to give the intermediate **I-5**. Then the intermediate **I-5** goes through the β-hydride elimination process to give the target product **15** and liberate the Pd(0). Noteworthily, the *N*,*N*-dimethylaminomethylferrocene **13** can be oxidized by O_2 to give *N*,*N*-dimethylaminomethylferrocenium, which can oxidize Pd(0) to regenerate Pd(II) for the next catalytic cycle.

In 2020, Cui, Wu and co-workers demonstrated that the planar chiral ferrocene structures could be achieved from the achiral ferrocenecarboxylic acid **16** with alkene **14** through a Pd(II)-catalyzed C–H alkenylation reaction (Scheme 10) [46]. The mono-protected amino acid **L8** was used as the single chiral ligand and the oxygen was used as the oxidant for this reaction. Both electron-donating and electron-withdrawing groups could be installed on the alkene substrate **14**, with the target planar chiral 2-alkenyl ferrocenecarboxylic acids **17** afforded in good to excellent enantioselectivities.

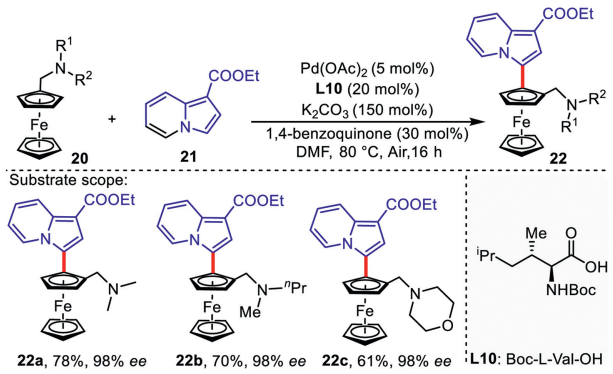
In 2019, You, Gu and co-workers demonstrated that the planar chiral ferrocene structures could be achieved from the achiral aminomethylferrocenes **13** and the oxazoles **18** through a Pd(II)-catalyzed asymmetric oxidative C–H/C–H cross-coupling reaction (Scheme 11) [47]. The mono-protected natural amino acid **L9** was used as the single chiral ligand and the 1,4-benzoquinone was used as the oxidant for this reaction. Oxazole and thiazoles bearing various functional groups worked well in this process, and the optically pure planar chiral ferrocene products were given in moderate to good yields. Mechanistically, the chiral amino acid and the palladium acetate could form the catalytically reactive complex, which could promote the C–H bond cleavage process of the aminomethylferrocene substrate **13** to generate the chiral Pd(II) intermediate **I-7**. Then, an electrophilic palladation of the azole substrate **18** into the intermediate **I-7** affords the intermediate **I-8**, which could go through a reductive elimination to afford the planar chiral product **19** and released a Pd(0) species. The Pd(0) is oxidized by air to regenerate Pd(II) for the next catalytic cycle.

In 2021, You and co-workers succeeded to use the indolizine derivative **21** as the arylation reagent to participate in the regio- and enantioselective C–H functionalization reaction of the aminomethylferrocene **20** (Scheme 12) [48]. The palladium acetate was used as the reaction catalyst in combination with the Boc-L-Val-OH (**L10**) used as the chiral ligand. The reaction exhibited good functional group tolerance on both the indolizine and the aminomethylferrocene substrates, with the corresponding arylated planar chiral aminomethylferrocene products afforded in good yields with excellent optical purities.

In 2019, You, Gu and co-workers reported an asymmetric cross-coupling reaction between the thiocarbonylferrocene **23** and the iodobenzene **24**, with the Rh(I) salt used as the re-



Scheme 11. Pd(II)-catalyzed cross-coupling reaction between ferrocenes and azoles.

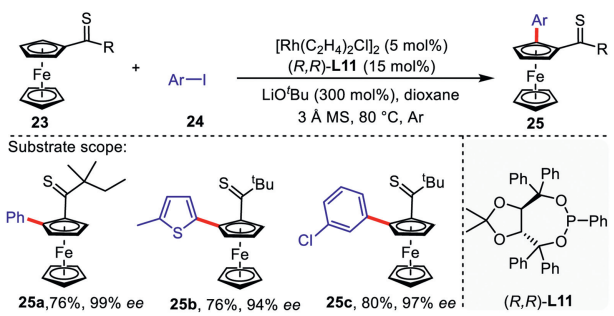


Scheme 12. Pd(II)-catalyzed cross-coupling reaction between dialkylaminomethylferrocenes and indolizines.

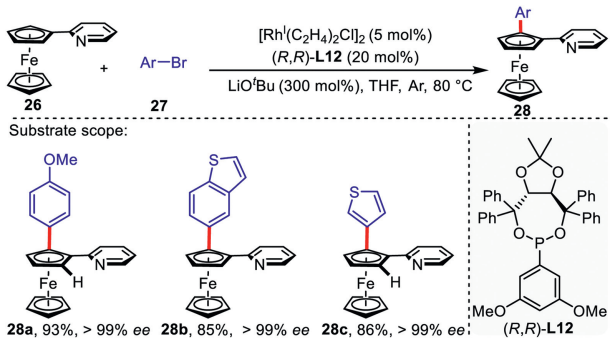
action catalyst and the (4*R*,5*R*)-(2,2-dimethyl-1,3-dioxolane-4,5-diyl)bis(diphenylmethanol) (TADDOL)-derived phosphonite (*R*,*R*)-**L11** used as the chiral ligand (Scheme 13) [49]. The reaction showed good functional group tolerance, with a diversity of aryl iodides and thiocarbonylferrocene substrates worked well to give the target planar chiral ferrocenes in good to excellent yields and enantioselectivity.

Soon later, the same group successfully adopted the aryl cross-coupling strategy in the enantioselective C–H arylation of ferrocenylpyridines (Scheme 14) [50]. The 2-pyridyl group on the ferrocene scaffold functionalized as a directing group to regio- and enantioselectively introduce the aryl group onto the *o*-position of the cyclopentadienyl ring under the promotion of the Rh(I)/(*R*,*R*)-**L12** catalytic system. Various aryl halides worked smoothly as the arylation reagent, with most of the *o*-substituted planar chiral ferrocenylpyridine products efficiently afforded as single enantiomers.

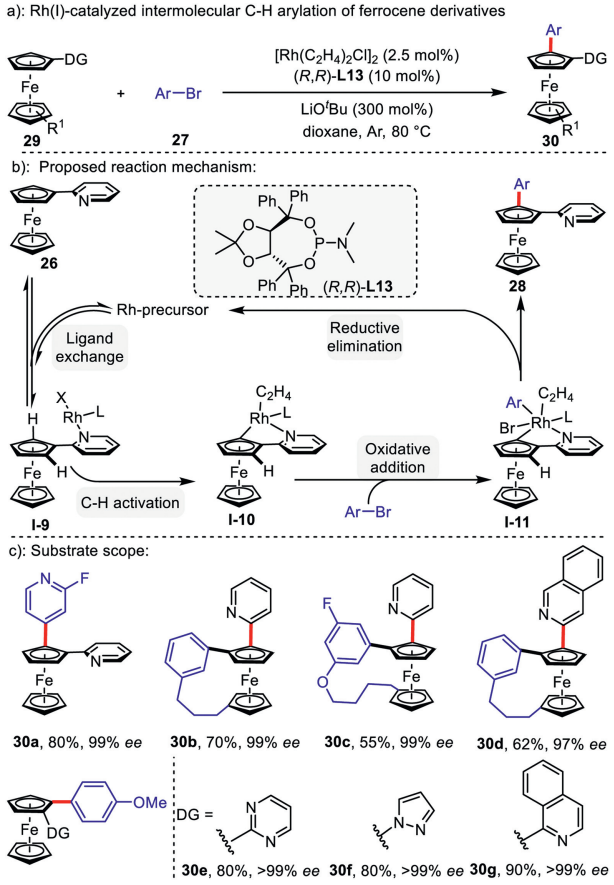
The authors intensively studied the reaction mechanism of the above C–H arylation of ferrocenylpyridines through both experimental and computational methods (Scheme 15) [51]. The



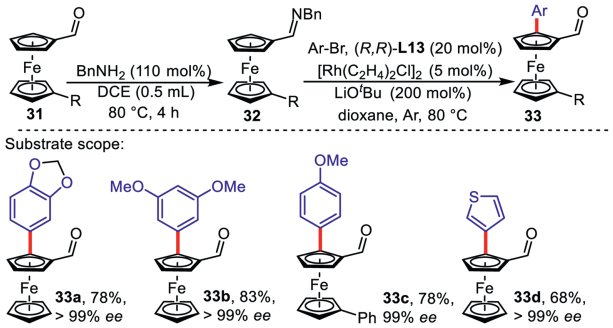
Scheme 13. Rh(I)-catalyzed thioketone-directed enantioselective C–H bond arylation of ferrocenes.



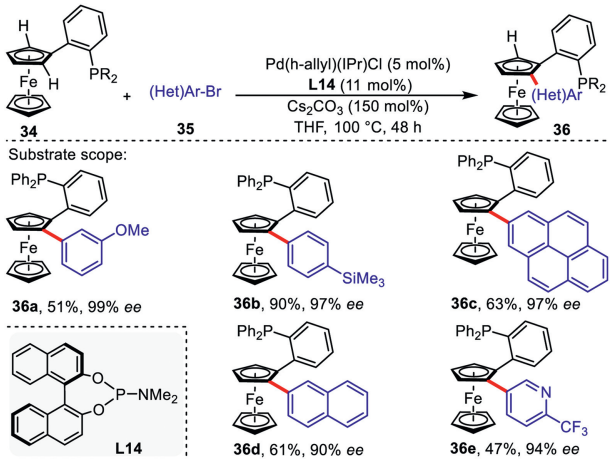
Scheme 14. Rh(I)-catalyzed coupling reaction to form planar chiral ferrocene-based pyridine derivatives.



Scheme 15. Rh(I)-catalyzed asymmetric C–H arylation reac-tion to form planar chiral ferrocenophanes.



Scheme 16. Rh(I)-catalyzed C–H arylation of ferrocenefor-maldehydes.

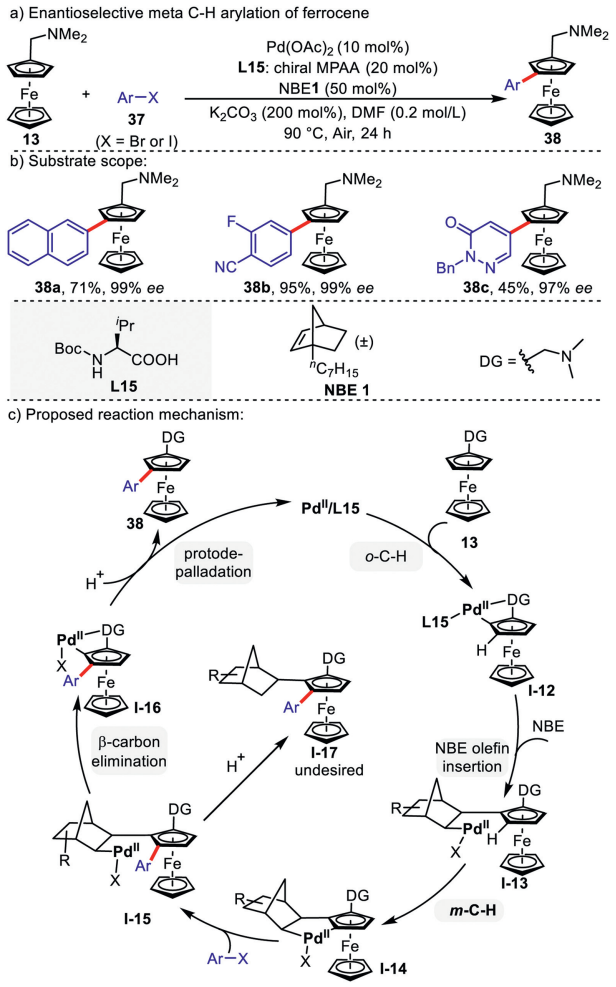


Scheme 17. Pd(II)-catalyzed and P(III)-directed asymmetric C–H arylation to form planar chiral ferrocenyl phosphines.

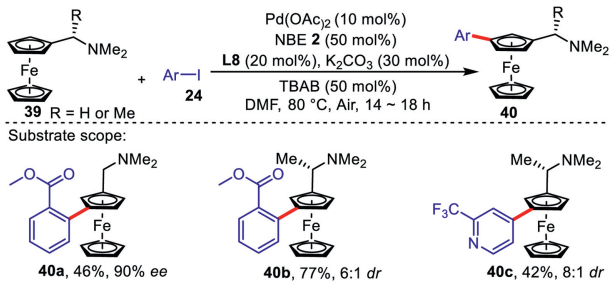
elementary steps in the catalytic cycle were elucidated, and the structures of several key intermediates were identified. The results revealed that the reaction initiates with the C–H activation of the ferrocene by the Rh(I)/(*R,R*)-**L13** complex *via* the intermediate **I-9**, followed by the oxidative addition of the intermediate **I-10** with aryl bromide to give the intermediate **I-11**. Reductive elimination of the Rh(I) catalyst from the intermediate **I-11** led to the formation of the final product. The final reductive elimination step is identified as the rate-limiting step of the catalytic cycle. Leveraging the mechanistic insights gained, the authors successfully utilized isoquinoline, pyrimidine, oxazoline, imidazole and pyrazole as the directing groups in this ferrocene *o*-C-H arylation protocol [6–8]-ferrocenophanes bearing unique molecular topology were efficiently afforded through this strategy in exclusive enantioselectivity.

In 2023, You's group discolsed an enantioselective arylation reaction of the commercially available ferroceneformaldehydes with aryl bromides (Scheme 16) [52]. The benzylamine was used to overcome the weak coordinating ability of the aldehyde group through *in situ* formation of the imine intermediate. With the Rh(I) used as the reaction catalyst and the phosphonite (*R,R*)-**L13** used as the chiral ligand, the arylated planar chiral ferroceneformaldehyde products could be formed in up to 83 % yield and as almost single enantiomers.

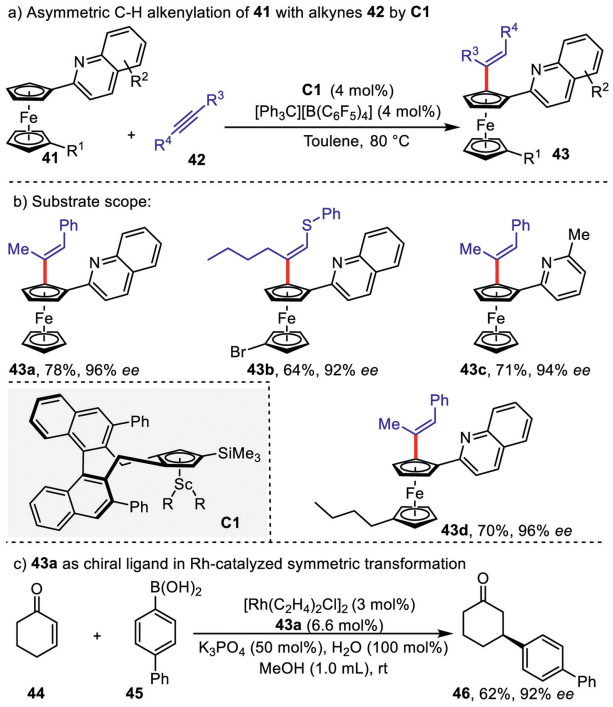
In 2024, Shi's group made a breakthrough in the facile preparation of planar chiral ferrocenyl phosphines (Scheme 17) [53]. They used the ferrocenyl phosphine **34** as the reaction substrate, with diverse aryl groups introduced to the *o*-position of the ferrocene moiety. The triarylphosphine group attached to the substrate **34** acted as an innovative directing group, which cooperated with the palladium catalyst and the chiral phosphine ligand **L14** to achieve



Scheme 18. Pd(II)-catalyzed enantioselective C–H activationto form 1,3-disubstituted planar chiral ferrocenes.



Scheme 19. Pd(II)-catalyzed enantioselective C3-arylation.



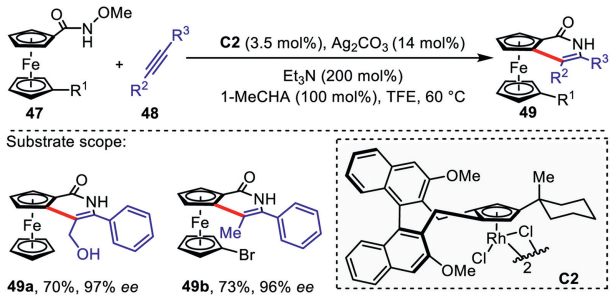
Scheme 20. Sc-catalyzed C–H alkenylation reaction between ferrocenes and alkynes.

both regio- and enantioselectivities during the ferrocene C–H activation reaction. A broad scope of functional groups could be tolerated on both the ferrocene substrate **34** and the arylbromide substrate **35**, and the planar chiral ferrocenyl phosphine products were facilely achieved in generally excellent optical purity.

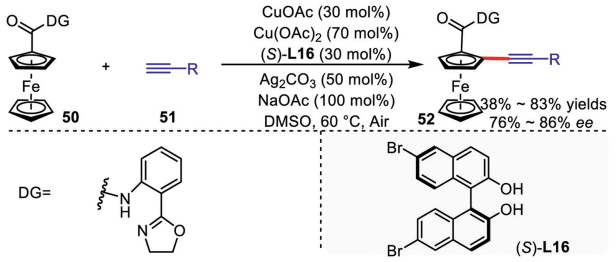
In 2023, Zhou's group succeeded in introducing an aryl group to the *m*-position of the ferrocene scaffold in both regio- and enantioselective fashion (Scheme 18a) [54]. An aminomethyl group was pre-installed on the ferrocene substrate **13** as the directing group. The $Pd(OAc)_2$ was used as the reaction catalyst, the mono-protected amino acid **L15** was used as the chiral ligand and the norbornene was used as the transent mediator. A diversity of aryliodides or arylbromides worked smoothly in this protocol as the aryl group donor, with the corresponding planar chiral 1,3-disubstituted ferrocene products **38** afforded in moderate to good yields as single enantiomers (Scheme 18b). The proposed mechanism involves the Pd(II)/**L15** complex-catalyzed, amino-directed regio-selective activation of the ferrocene *o*-C-H bond, followed by the insertion of norbornene to generate the intermediate **I-13**. Then the *m*-C-H bond of the ferrocene substrate could be activated through the formation of the intermediate **I-14**, which could go through oxidative addition with the aryl halide substrate **37** and reductive elimination of the Pd(II) complex to give the intermediate **I-15**. Then a β-carbon elimination process within the intermediate **I-15** extrudes the norbornene moiety and gives the intermediate **I-16**, which can produce the final product **38** *via* a protode-palladation step and liberate the This strategic placement of the Pd(II) catalyst at the 3-position enables the of electrophiles and subsequent reductive elimination, thereby establishing the critical *meta* C–C bond. The catalytic cycle is completed through β-carbon elimination, which liberates the NBE **1** mediator, followed by the depalladation of intermediate **I-16**, leading to the release of the final product **38** and regenerate the Pd(II)/**L15** complex for additional catalytic cycles (Scheme 18c).

In 2024, Kapur, Madhavan and co-workers reported a Pd(II)-catalyzed regio- and stereoselective distal C–H activation of the chiral *N*,*N*-dimethyl-1-ferrocenylethylamine **39** with various aryl iodides **24** (Scheme 19) [55]. The chiral *N*-acetyl phenylalanine **L8** and the NBE **2** were used as the dual ligands in combination with the $Pd(OAc)_2$ catalyst for this reaction. A broad range of ferrocene-1,3-derivatives featuring both central and planar chirality, with varying substituents, were synthesized in good to excellent yields with high enantio– or diastereoselectivities.

In 2021, Hou and Luo's group reported a highly enantioselective C–H alkenylation reaction of quinoline-substituted ferrocene **41** with alkynes **42** using scandium complex **C1** as the chiral catalyst (Scheme 20a) [56]. A series of *o*-alkenylated planar-chiral ferrocenyl quinoline products were afforded in good to excellent yields and optical purity (Scheme 20b). It was attractive that no atoms were lost during the catalytic reaction, and the planar chiral ferrocene products obtained from this protocol could be applied as



Scheme 21. Rh(III)-catalyzed C–H cycloaddition reaction between ferrocenecarboxamides and internal alkynes.



Scheme 22. Cu-mediated enantioselective C–H activation reaction to form planar chiral ferrocenophanes.

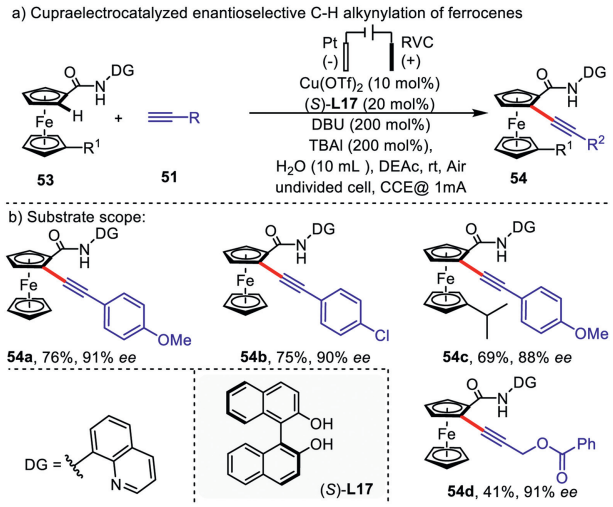
chiral ligand for the asymmetric rhodium-catalyzed hydroarylation of the cyclohexanone (Scheme 20c).

In 2022, You, Zheng and co-workers reported a Rh(III)-catalyzed enantioselective C–H activation/annulation reaction of substituted ferrocenecarboxamides with internal alkynes (Scheme 21) [57]. The chiral CpRh(III) complex **C2** was used as the reaction catalyst, yielding the planar chiral ferrocene-fused pyridone products in moderate to excellent yields and enantioselectivities.

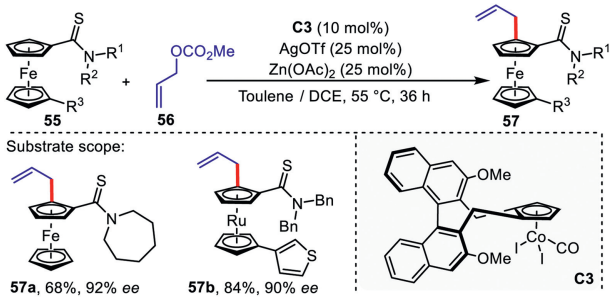
In 2023, Yu, Wang and co-workers reported a Cu-mediated enantioselective ferrocene C–H alkynylation reaction with terminal alkynes (Scheme 22) [58]. The chiral DDBINOL derivative (*S*)-**L16** was used as the ligand for the enantioselective induction during the oxidative cross-coupling process. An oxazoline-aniline group was pre-installed on the ferrocene scaffold as the directing group, introducing the external alkynyl groups onto the *o*-position of the ferrocene moiety.

In 2024, Shi, Yao and co-workers reported a novel copper-catalyzed enantioselective *o*-C-H alkynylation reaction of ferrocene carboxamides (Scheme 23a) [59]. The 8-aminoquinoline in the amide moiety of the substrate **53** was adopted as the directing group for the *o*-induction of the alkynyl group with the promotion of the copper catalyst and the chiral BINOL ligand (*S*)-**L17**. Both electron-donating and electron-withdrawing groups could be installed on the arylalkyne substrate **51**, with the target planar chiral alkynyl ferrocenes **54** afforded in good to excellent enantioselectivities. Noteworthily, the stoichiometric external oxidant TBHP that used for the oxidative C–H cross coupling process could be replaced with renewable electricity (Scheme 23b). The asymmetric reaction between the substrates **53** and **51** could be carried out under electrochemical conditions in an undivided cell in presence of the same copper catalyst and chiral ligand. The corresponding products were generally afforded in higher yields without much loss of the optical purity.

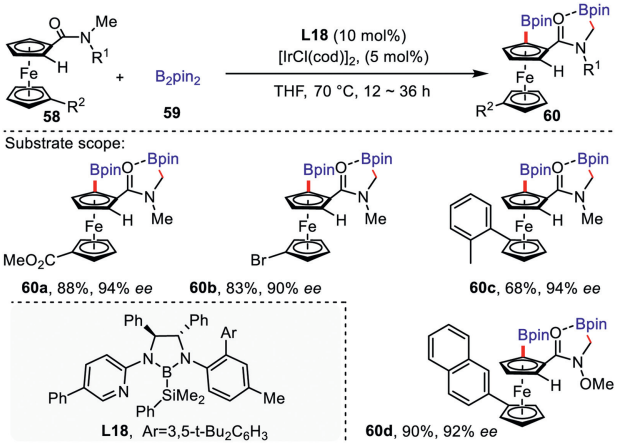
In 2024, You, Zheng and co-workers reported a cobalt-catalyzed asymmetric C(sp^2)-C(sp^3) cross-coupling reaction between the ferrocene thioamides **55** and the allyl carbonates **56** for the facile preparation of enantio–enriched *o*-allyl substituted ferrocene thioamide products **57** (Scheme 24) [60]. The binaphthyl-based chiral cobalt complex **C3** was used as the reaction catalyst and the



Scheme 23. Cu(II)-catalyzed enantioselective C–H alkynylation reaction to form planar chiral ferrocene carboxamides.



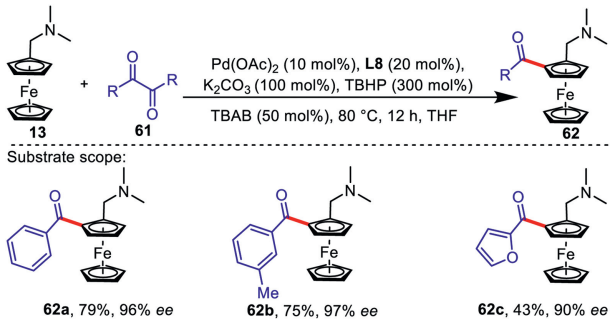
Scheme 24. Co-catalyzed the coupling reaction to form planar chiral allylation products.



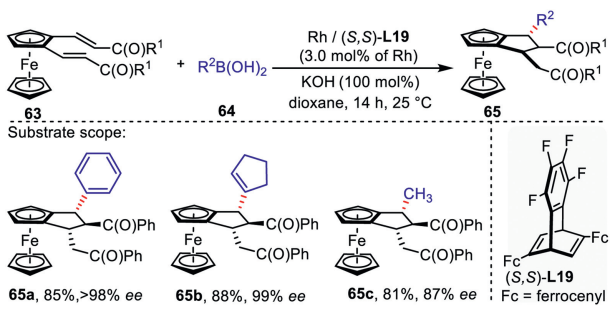
Scheme 25. Rh(I)-catalyzed asymmetric C–H arylation reaction to form planar chiral ferrocenophanes.

target products were given in up to 81% yield and 95% *ee* value. Noteworthily, the iron center in the ferrocene structure could also be switched into a ruthenium atom.

In 2022, Xu, Ke and colleagues achieved the enantioselective dual borylation of ferrocenes through an amide-directed iridium-catalyzed C–H activation reaction (Scheme 25) [61]. The chiral bidentate boryl ligand **L18** was used in combination with the Ir(I) catalyst, and a series of planar chiral borylated ferrocene products bearing various substituents were afforded in good to excellent yields and optical purity. Mechanistic studies demonstrate that the



Scheme 26. Pd(II)-catalyzed enantioselective C–H direct acylation of ferrocene derivatives.



Scheme 27. Rh-catalyzed the desymmetric cyclization reaction to form planar and central chirality in metallocenes.

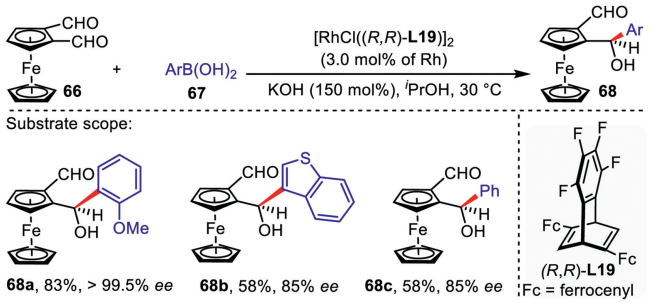
C–H borylation of the *N*-methyl group in the amide moiety plays a crucial role in enhancing enantioselectivity.

In 2014, Cui, Wu and co-workers reported a Pd(II)-catalyzed enantioselective C–H activation of *N*,*N*-dimethylaminomethylferrocene **13** with diphenyl diketone **61** (Scheme 26) [62]. The chiral amino acid ligand **L8** was used in combination with the Pd(II) catalyst, and a series of planar chiral 2-acyl-1-dimethylaminomethylferrocene products were afforded in good to excellent yields and optical purity. The afforded products could be easily converted to various chiral ligands *via* simple trans-formations.

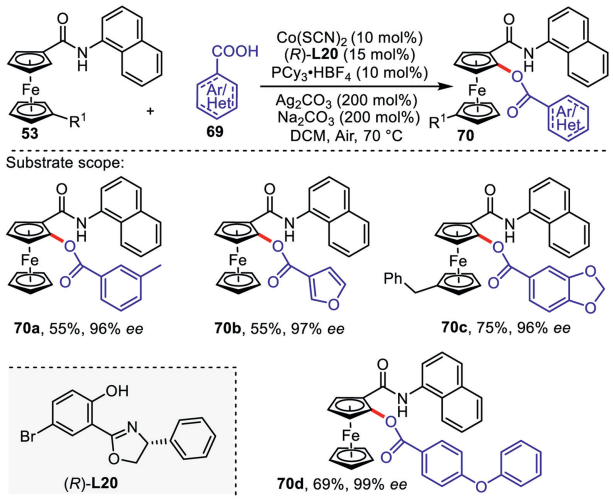
In 2023, Ming, Chen and co-workers reported a Rh-catalyzed conjugate addition/cyclization cascade reaction between the symmetric ferrocene diketone substrate **63** and the organoboronic acid **64** for access to the ferrocene-fused cyclopentane molecules bearing both planar and central chirality (Scheme 27) [63]. The chiral ferrocene-derived diene molecule (*S*,*S*)-**L19** was used as the ligand to achieve high efficiencies and selectivities. A diversity of substituents and substitution patterns were well tolerated on the organoboronic acid substrates, with the ferrocene-fused cyclopentane products afforded in good to excellent yields and optical purity as single diastereomers.

In 2025, Ming and co-workers reported a Rh-catalyzed asymmetric aryl addition reaction between the 1,2-diformylferrocene **66** and the arylboronic acid **67** (Scheme 28) [64]. The chiral (*R*,*R*)-**L19** was used as the ligand for this reaction. A broad scope of planar-chiral formylferroccene products with different substituents were afforded in good to excellent yields and enantioselectivities.

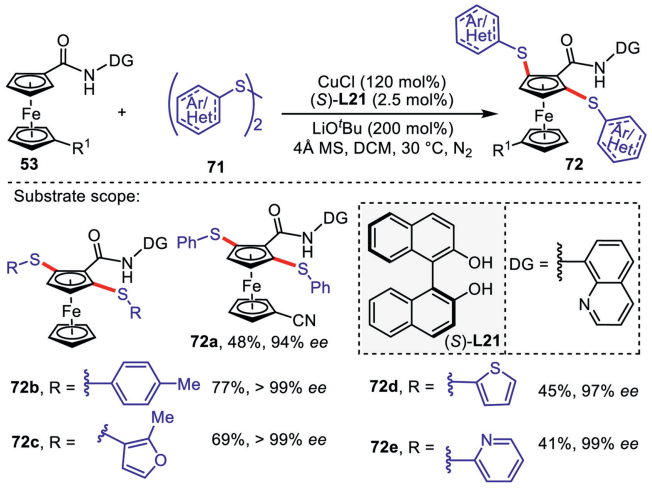
In 2024, Shi, Yao and co-workers reported a cobalt-catalyzed enantioselective C–H acyloxylation of the ferrocene amides **53** with various carboxylic acids **69** (Scheme 29) [65]. The chiral salicyloxazoline (*R*)-**L20** and the *in situ*-formed tricyclohexylphosphine oxide were used as the dual ligands in combination with the $Co(SCN)_2$ catalyst for this dehydrogenative C–H acyloxylation reaction. The planar chiral *o*-acyloxylated ferrocene amide products bearing various substitution patterns were afforded in moderate to good yields with excellent optical purity.



Scheme 28. Rh-catalyzed asymmetric addition of the 1,2-diformylmetallocenes.

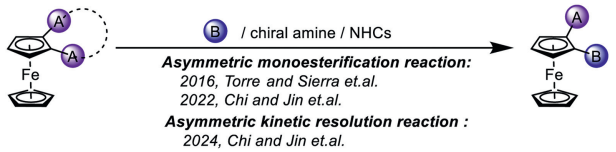


Scheme 29. Co-catalyzed enantioselective C–H acyloxylation reaction to form oxy-substituted planar chiral ferrocenes.

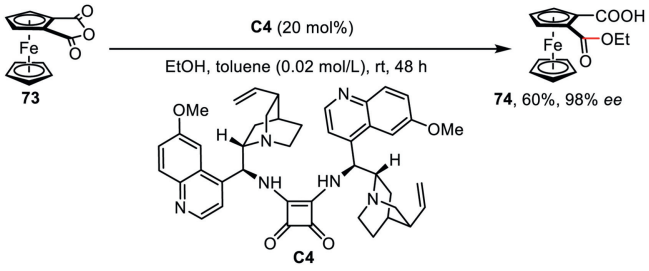


Scheme 30. Cu(I)-catalyzed enantioselective C–H thiolation of ferrocenes.

In 2025, Shi and colleagues reported a copper-mediated enantioselective C–H thiolation of ferrocenes *via* a Cu(I)-catalyzed C–H activation process (Scheme 30) [66]. The reaction used a chiral 1,1′-bi-2,2′-naphthol ligand (*S*)-**L21** in combination with a Cu(I) catalyst, enabling the synthesis of a diverse array of planar chiral sulfur-substituted ferrocenes with various substituents. The products were obtained in good to excellent yields with high optical purity, highlighting the efficacy of the catalytic system and expanding the synthetic toolbox for access to chiral organosulfur compounds.



Scheme 31. Asymmetric organocatalysis for the synthesis of planar chiral ferrocenes.



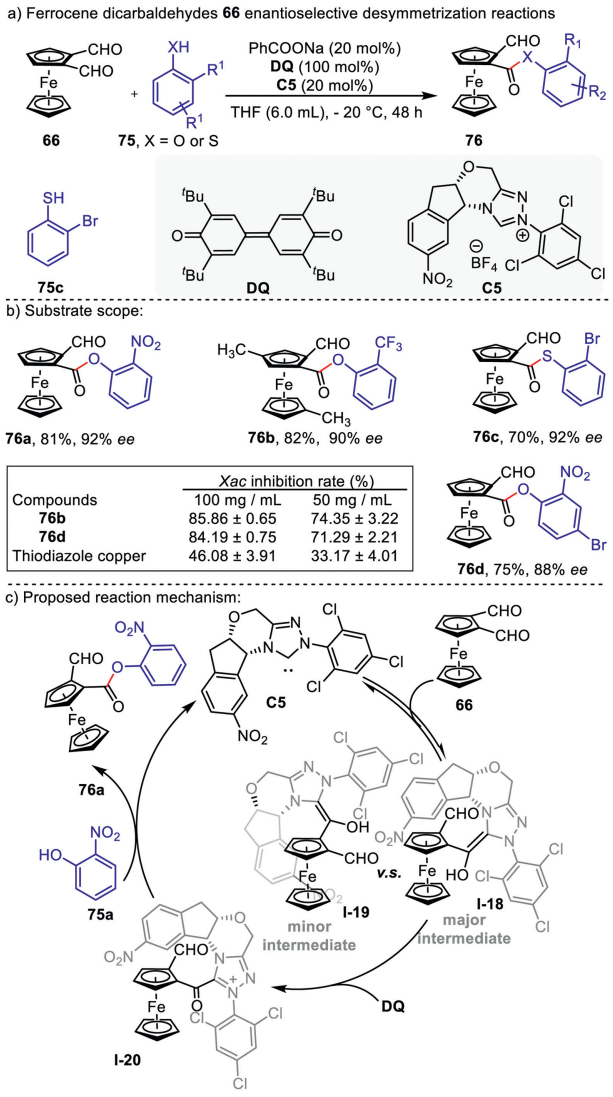
Scheme 32. Organocatalytic desymmetrization of *meso*–ferrocene anhydride.

3. Organocatalyzed planar chiral ferrocene syntheses

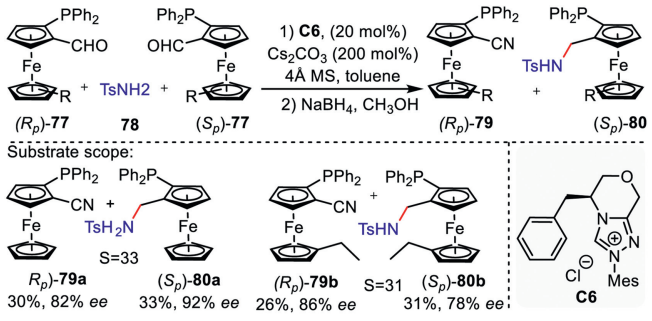
The field of organocatalytic synthesis of planar chiral ferrocene derivatives is still in its infancy. Researchers have explored the use of chiral amines and *N*-heterocyclic carbenes (NHCs) as organocatalysts for asymmetric monoesterification and kinetic resolution strategies (Scheme 31).

In currently, the constructions of planar chiral ferrocenes *via* organocatalytic methods have been relatively less developed. In 2016, Torre, Sierra and co-workers disclosed an asymmetric monoesterification reaction of the *meso*–ferrocene anhydride **73** (Scheme 32) [67]. Chiral bifunctional organic catalysts bearing both an amino group and an H-bond donor fragment were evaluated for this desymmetric esterification process. The planar chiral ferrocenyl dicarboxylic acid mono ethylate product **74** could be afforded in up to 98% *ee* value under the catalysis of the quinine-derived squaramide catalyst **C4**.

N–Heterocyclic carbenes (NHCs) have also been applied as effective catalysts in the desymmetric mono-esterification reactions of ferrocene derivatives [68–71]. In 2022, Chi, Jin and co-workers reported the NHC-catalyzed oxidative mono-esterification reaction of diformylferrocenes **66** with electron-deficient phenols **75** (Scheme 33) [72]. The chiral NHC **C5** was used as the reaction catalyst and the diphenoquinone (DQ) was used as the external oxidant. Electron-withdrawing groups were well tolerated on the phenol substrate **75** to give the planar chiral ferrocene monoester products **76** in good to excellent yields and enantioselectivities. Electron-donating and electron-neutral groups led to little formation of the desired products under the current catalytic condition. However, the phenol substrates **75** could be replaced with mercaptans **75c** to give the ferrocene mono-thioesters **76c** in satisfactory results under the same catalytic condition, regardless of the substitution patterns of the mercaptan scaffolds. The possible mechanism was briefly illustrated as shown in Scheme 33c. The addition of the chiral NHC **C5** to the ferrocene dicarbaldehyde **66** gives two diastereomeric intermediates **I-18** and **I-19** in reversible fashion. Due to steric hindrance, the intermediate **I-18** is more easily formed than the intermediate **I-19** and can be oxidized under mild conditions to give the intermediate **I-20**. Then, nucleophiles such as phenols and mercaptans can react with the intermediate **I-20** to ultimately yield the planar chiral product **76a** or **76c**, liberating the NHC catalyst and completing the cycle. *In vitro* inhibitive activities of the planar chiral products **76** against *Xanthomonas axonopodis* pv. *citri* (*Xac*) have been examined. The products **76b** (100 μg/mL) and **76d** (100 μg/mL) exhibited *Xac* inhibition rate of 85.86% ± 0.65% and 84.19% ± 0.75%, which were better than that of the thiodiazole copper (46.08% ± 3.91%) (Scheme 33b).



Scheme 33. NHC-catalyzed desymmetrization of ferrocene-derived dicarbaldehydes.



Scheme 34. NHC-catalyzed a kinetic resolution process to form ferrocene-derived phosphine carbonitrile and phosphinesulfonamide.

Recently, the same group reported an NHC-catalyzed kinetic resolution reaction of the racemic ferrocenyl carbaldehyde substrate **77** bearing a phosphinyl group (Scheme 34) [73]. The toluenesulfonamide **78** ($TsNH_2$) was used as the N source to con-

vert the aldehyde group into the cyanide group through a cascade amide formation/de-sulfination process. The ferrocenyl nitriles (R_p)-**79** were generally afforded in good yields and optical purity. Meanwhile, the $NaBH_4$ was added at the end of this reaction to reduce the unreacted imine intermediate into the Ts-protected ferrocenylmethylamines (S_p)-**80**. It was interesting to find that the afforded planar chiral ferrocene derivatives showed promising antibacterial bioactivities against the bacterial plant pathogens.

4. Summary and outlook

The development of catalytic methods for facile and enantioselective construction of planar chiral ferrocene-based multifunctional molecules has received considerable interest in the recent decade. Transition metal-catalysis has been dominating in the desymmetrization of mono-substituted ferrocene structures. Asymmetric ferrocene C(sp^2)-H activation reactions have been extensively studied in the transition metal-catalyzed planar chiral ferrocene synthesis. The pre-installation of suitable directing groups and the design of effective chiral ligands are critical for the regio- and stereoselectivities in these transformations. Organic catalysts such as chiral amines and NHCs have recently been used to promote the enantioselective desymmetrization and kinetic resolution of ferrocene derivatives. The introduction of suitable electron-withdrawing functional groups onto the ferrocene structures and the selection of suitable nucleophilic organic catalysts have played crucial roles in the organocatalytic ferrocene synthesis. Based on the abundant catalytic methods developed in the recent decade, diverse planar chiral ferrocene molecules bearing alkyl, aryl, heteroaryl, alkenenyl, alkynyl, and other functional groups have been efficiently obtained in optically enriched forms.

However, challenges and limitations remain in the asymmetric catalytic synthesis of planar chiral ferrocenes. The reaction modes have long been dominated by transition metal-catalyzed C(sp^2)-H activations. Asymmetric additions, oxidations, hydrogenations and substitution reactions have been relatively less developed in the construction of planar chiral ferrocenes. Most of C(sp^2)-H activation reactions in planar chiral ferrocenes have taken place on the *o*-position to the directing groups, with limited success in the *m*-selective C(sp^2)-H activation of ferrocene structures. Comparing with the transition metal catalysis, organocatalytic reactions have been rarely used in the asymmetric synthesis of ferrocene derivatives.

Therefore, great efforts are still needed in the development of efficient and stereoselective catalytic methods for planar chiral ferrocene synthesis. For instance, the introduction of novel directing groups with practical synthetic significance represents an interesting strategy in the stereoselective ferrocene functionalization. The development of novel catalytic systems to realize novel reaction modes and further enhance the reaction selectivity is still of great significance in this research field. Multi-component cascade reactions, co-operative catalysis with different catalysts and relay activations may bring new breakthroughs to the construction of planar ferrocene derivatives. The development of novel catalytic methods will undoubtedly further promote the application of planar chiral ferrocene derivatives in drug development and material sciences.

Declaration of competing interest

The authors declare that they have no known competing financial interests or personal relationships that could have appeared to influence the work reported in this paper.

CRediT authorship contribution statement

Haitao Liu: Writing – original draft. **Youlin Deng:** Investigation. **Dan Ling:** Investigation. **Lingzhu Chen:** Writing – review & editing. **Zhichao Jin:** Writing – review & editing.

Acknowledgments

We acknowledge the financial support from the National Key Research and Development Program of China (No. 2022YFD1700300). National Natural Science Foundation of China (Nos. 22371057, 32172459). The Central Government Guides Local Science and Technology Development Fund Projects [Qiankehezhongyindi (2024)007, (2023)001]. The Program of Major Scientific and Technological, Guizou Province [Qiankehechengguo(2024)zhongda007]. Yongjiang Plan for Innovation and Entrepreneurship Leading Talent Project in the City of Nanning (No. 2021005). The 10 Talent Plan (Shicengci) of Guizhou Province (No. [2016]5649). The Program of Introducing Talents of Discipline to Universities of China (111 Program, D20023) at Guizhou University.

References

[1] A. Rabti, N. Raouafi, A. Merkoçi, Carbon 108 (2016) 481–514.
[2] M. Gallei, C. Rüttiger, Chem. Eur. J. 24 (2018) 10006–10021.
[3] Z. Huang, H. Yu, L. Wang, et al., Coord. Chem. Rev. 430 (2021) 213737.
[4] D. Astruc, Chem. Commun. 59 (2023) 7321–7345.
[5] T.J. Colacot, Chem. Rev. 103 (2003) 3101–3118.
[6] A. Singh, I. Lumb, V. Mehra, V. Kumar, Dalton Trans. 48 (2019) 2840–2860.
[7] L.V. Snegur, A.A. Simenel, A.N. Rodionov, V.I. Boev, Russ. Chem. Bull. 63 (2014) 26–36.
[8] M. Patra, G. Gasser, Nat. Rev. Chem. 1 (2017) 0066.
[9] B. Sharma, V. Kumar, J. Med. Chem. 64 (2021) 16865–16921.
[10] L.V. Snegur, V.N. Babin, A.A. Simenel, et al., Russ. Chem. Bull. 59 (2010) 2167–2178.
[11] A. Sun, J. Lin, C. Pi, R. Xu, X. Cui, Arch. Pharm. Chem. Life Sci. 349 (2016) 186–192.
[12] R. Wang, H. Chen, W. Yan, et al., Eur. J. Med. Chem. 190 (2020) 112109.
[13] A. Chaudhary, K. Poonia, Inorg. Chem. Commun. 134 (2021) 109044.
[14] L. Zeng, M. Tang, C. Pi, et al., Cancers 13 (2021) 4677.
[15] J. Zheng, L. Zeng, M. Tang, et al., Int. J. Mol. Sci. 22 (2021) 3097.
[16] M.Čakić Semenčić, L. Barišić, Croat. Chem. Acta 90 (2017) 537–569.
[17] Z.H. Chohan, A. Scozzafava, C.T. Supuran, J. Enzyme Inhib. Med. Chem. 17 (2008) 261–266.
[18] B.S. Ludwig, J.D.G. Correia, F.E. Kühn, Coord. Chem. Rev. 396 (2019) 22–48.
[19] Y. Deng, H. Cai, J. Jin, et al., J. Agric. Food Chem. 72 (2024) 11917–11927.
[20] L.X. Dai, T. Tu, S.L. You, W.P. Deng, X.L. Hou, Acc. Chem. Res. 36 (2003) 659–667.
[21] R.C.J. Atkinson, V.C. Gibson, N.J. Long, Chem. Soc. Rev. 33 (2004) 313–328.
[22] R. Gómez Arrayás, J. Adrio, J.C. Carretero, Angew. Chem. Int. Ed. 45 (2006) 7674–7715.
[23] T. Noël, J. Van der Eycken, Green Process. Synth. 2 (2013) 297–309.
[24] J.C. Zhu, D.X. Cui, Y.D. Li, et al., ChemCatChem 10 (2018) 907–919.
[25] K. Yoshida, R. Yasue, Chem. Eur. J. 24 (2018) 18575–18586.
[26] D. Xu, J. Zhang, L. Dai, ChemistrySelect 5 (2020) 9443–9456.
[27] L. Cunningham, A. Benson, P.J. Guiry, Org. Biomol. Chem. 18 (2020) 9329–9370.
[28] T. Izumi, F. Tamura, K. Sasaki, Bull. Chem. Soc. Jpn. 65 (2006) 2784–2788.
[29] M. Ogasawara, S. Watanabe, L. Fan, K. Nakajima, T. Takahashi, Organometallics 25 (2006) 5201–5203.
[30] A.N.R. Alba, R. Rios, Molecules 14 (2009) 4747–4757.
[31] M. Ogasawara, S. Arae, S. Watanabe, K. Nakajima, T. Takahashi, ACS Catal. 6 (2016) 1308–1315.
[32] L.F. Battelle, R. Bau, G.W. Gokel, R.T. Oyakawa, I.K. Ugi, J. Am. Chem. Soc. 95 (1973) 482–486.
[33] F. Rebière, O. Riant, L. Ricard, H.B. Kagan, Angew. Chem. Int. Ed. 32 (1993) 568–570.
[34] M. Tsukazaki, M. Tinkl, A. Roglans, et al., J. Am. Chem. Soc. 118 (1996) 685–686.
[35] R. Peters, D.F. Fischer, Org. Lett. 7 (2005) 4137–4140.
[36] C. Genet, S.J. Canipa, P. O'Brien, S. Taylor, J. Am. Chem. Soc. 128 (2006) 9336–9337.
[37] D.W. Gao, Q. Gu, C. Zheng, S.L. You, Acc. Chem. Res. 50 (2017) 351–365.
[38] R. Deng, Y. Huang, X. Ma, et al., J. Am. Chem. Soc. 136 (2014) 4472–4475.
[39] B.B. Xu, J. Ye, Y. Yuan, W.L. Duan, ACS Catal. 8 (2018) 11735–11740.
[40] L. Liu, H. Liu, Z. Zuo, et al., Chin. Chem. Lett. 32 (2021) 239–242.
[41] G. Xu, C.H. Senanayake, W. Tang, Acc. Chem. Res. 52 (2019) 1101–1112.
[42] Q.W. Zhang, K. An, L.C. Liu, Y. Yue, W. He, Angew. Chem. Int. Ed. 54 (2015) 6918–6921.
[43] A. Urbano, G. Hernández Torres, A.M. del Hoyo, A. Martínez Carrión, M. Carmen Carreño, Chem. Commun. 52 (2016) 6419–6422.

[44] Q. Zhou, L. Qiao, A.A. Zhang, et al., Green Synth. Catal. 6 (2025) 198–201.
[45] C. Pi, Y. Li, X. Cui, et al., Chem. Sci. 4 (2013) 2675–2679.
[46] Y. Huang, C. Pi, X. Cui, Y. Wu, Adv. Synth. Catal. 362 (2020) 1385–1390.
[47] Z.J. Cai, C.X. Liu, Q. Gu, C. Zheng, S.L. You, Angew. Chem. Int. Ed. 58 (2019) 2149–2153.
[48] C.X. Liu, W.W. Zhang, P. Yang, et al., Chem Catal. 2 (2022) 102–113.
[49] Z.J. Cai, C.X. Liu, Q. Wang, Q. Gu, S.L. You, Nat. Commun. 10 (2019) 4168.
[50] C.X. Liu, Z.J. Cai, Q. Wang, et al., CCS Chem. 2 (2020) 642–651.
[51] C.X. Liu, P.P. Xie, F. Zhao, et al., J. Am. Chem. Soc. 145 (2023) 4765–4773.
[52] C.X. Liu, F. Zhao, Q. Gu, S.L. You, ACS Cent. Sci. 9 (2023) 2036–2043.
[53] X. Lv, M. Wang, Y. Zhao, Z. Shi, J. Am. Chem. Soc. 146 (2024) 3483–3491.
[54] L. Zhou, H.G. Cheng, L. Li, et al., Nat. Chem. 15 (2023) 815–823.
[55] P. Gupta, P.C. Tiwari, S. Madhavan, M. Kapur, ACS Catal. 14 (2024) 17460–17468.
[56] S.J. Lou, Q. Zhuo, M. Nishiura, G. Luo, Z. Hou, J. Am. Chem. Soc. 143 (2021) 2470–2476.
[57] Q. Wang, Y.H. Nie, C.X. Liu, et al., ACS Catal. 12 (2022) 3083–3093.
[58] X. Kuang, J.J. Li, T. Liu, et al., Nat. Commun. 14 (2023) 7698.
[59] Z.Z. Zhang, G. Zhou, Q. Yue, Q.J. Yao, B.F. Shi, ACS Catal. 14 (2024) 4030–4039.
[60] Y. Zheng, P.P. Xie, C. Zheng, S.L. You, CCS Chem. (2024) 1–14.
[61] X.L. Zou, Y.W. Li, Z.F. Ke, S.M. Xu, ACS Catal. 12 (2022) 1830–1840.
[62] C. Pi, X. Cui, X. Liu, et al., Org. Lett. 16 (2014) 5164–5167.
[63] Y. Yang, N.N. Hang, H.Y. Liu, S. Chen, J. Ming, ACS Catal. 13 (2023) 12464–12471.
[64] N.N. Hang, E.G. Tong, T. Qi, C. Sun, J. Ming, Chem. Sci. 16 (2025) 5880–5886.
[65] F.R. Huang, P. Zhang, Q.J. Yao, B.F. Shi, CCS Chem. 6 (2024) 2783–2793.
[66] J.Y. Ma, Q.J. Yao, L.C. Jiang, et al., J. Am. Chem. Soc. 147 (2025) 7061–7069.
[67] C. Valderas, L. Casarrubios, M.C. de la Torre, M.A. Sierra, Tetrahedron Lett. 58 (2017) 326–328.
[68] M. Zhang, X. Yang, X. Peng, X. Li, Z. Jin, Sci. China Chem. 68 (2024) 815–825.
[69] J. Lv, Y. Nong, K. Chen, et al., Chin. Chem. Lett. 34 (2023) 107570.
[70] X. Yang, H. Wang, Z. Jin, Y.R. Chi, Green Synth. Catal. 2 (2021) 295–298.
[71] Y. Zhang, H. Cai, X. Gan, Z. Jin, Sci. China Chem. 67 (2023) 482–511.
[72] X.K. Lv, J. Xu, C.Y. Sun, et al., ACS Catal. 12 (2022) 2706–2713.
[73] Y. Lv, C. Mou, Q. Liu, et al., Org. Lett. 26 (2024) 1584–1588.